Bona fide alveolar macrophage generation from long-term *in vitro* culture of fetal precursors provides a novel platform for gene therapy and functional studies

Fengqi Li[1, #], Katarzyna Okreglicka[1, #], Lea Pohlmeier[1], Christoph Schneider[1,2], Manfred Kopf[1, *]

[1]Institute of Molecular Health Sciences, Department of Biology, ETH Zürich, Switzerland.
[2]Institute of Physiology, University of Zürich, Switzerland.

[#]These authors contributed equally to this work.

*Correspondence: manfred.kopf@ethz.ch

ABSTRACT

Tissue-resident macrophage (MΦTR)-based immune therapies have been proposed for various diseases. However, it is still a challenge to generate a considerable amount of MΦTR that possess tissue-specific functions. Here we show that fetal liver monocytes (FLiMo) cultured with GM-CSF (also known as CSF2) rapidly differentiate into a long-lived, homogeneous alveolar macrophage (AM)-like population *in vitro.* CSF2-cultured FLiMo (CSF2-cFLiMo) remain the capacity to develop into *bona fide* AM upon transfer into *Csf2ra*$^{-/-}$ neonates and prevent development of alveolar proteinosis for at least 1 year *in vivo*. Compared to bone marrow-derived macrophages (BMM), CSF2-cFliMo more efficiently engraft empty AM niches in the lung and protect mice from influenza virus infection. Notably, to harness the potential of this approach for gene therapy, we restored a disrupted Csf2ra gene in FLiMo and their capacity to develop into AM *in vivo*, by retroviral expression of a wild-type gene. Taken together, we provide a novel platform for high-throughput genetic manipulation of AM that can be used for biological and therapeutic studies.

Key words: Alveolar macrophages, Fetal liver monocytes, Gene therapy

Introduction

Tissue-resident macrophages (MΦTR) are heterogeneous cell populations, present in almost all tissues and play multiple tissue-specific functions in homeostasis and diseases[1, 2]. MΦ-based therapies have been proposed as potential strategies in various diseases[3, 4, 5].

Lung resident AM play important roles in host defense to pulmonary infections and non-inflammatory clearance of inhaled particles[6]. Moreover, AM are required for catabolism of surfactant and removal of apoptotic cells and cellular debris that otherwise accumulate in the alveoli resulting in impaired air exchange[7]. AM are derived from late EMP and fetal liver monocytes, which colonize the lung during late embryogenesis, and are maintained life-long by self-renewal after birth[8, 9]. Development and expansion are driven perinatally by GM-CSF-induced PPARγ[10, 11]. Accordingly, absence of PPARγ, GM-CSF or one of the GM-CSFR subunits, Csf2ra and Csf2rb, in mice results in abrogated AM development and pulmonary alveolar proteinosis (PAP)[10, 11, 12, 13, 14]. Similarly, mutations in *CSF2RA* and *CSF2RB* genes have been identified in human PAP patients, which is associated with long-term respiratory insufficiency and high susceptibility to microbial infection[15, 16, 17].

It has been shown that pulmonary transplantation of BMM or induced pluripotent stem cell (iPSC)-derived MΦ to *Csf2rb*$^{-/-}$ mice can prevent development of PAP[18, 19, 20, 21]. However, whether these transplanted MΦ resemble *bona fide* self-renewing AM with functional capacities beyond surfactant clearance remains unclear. Here, we have established a biologically relevant model to study AM development and function by gene editing *in vitro* and assessment of functional consequences *in vivo*. By culturing purified fetal liver monocytes with GM-CSF, we were able to generate high numbers of AM-like MΦ that can be kept proliferating like stem cells *in vitro* for several months and possess the ability to restore AM development and function upon intranasal transfer to *Csf2ra*$^{-/-}$ neonates. GM-CSF-cultured fetal liver monocytes (CSF2-cFLiMo) resemble *bona fide* AM in gene expression profile, surface markers, and functional capacities including potent self-renewal capacity, clearance of surfactant, and efferocytosis of apoptotic cells during influenza virus infection. In contrast to BMM, CSF2-cFliMo more efficiently engraft empty AM niches and protect mice from influenza infection. Finally, CSF2RA re-expression in *Csf2ra*$^{-/-}$ FLiMo by retroviral gene transfer restored their potential to develop into *bona fide* AM. Altogether, this platform provides a potent platform to study genes involved in AM development and function, as well as for therapeutic approaches.

Results

In vitro GM-CSF-differentiated fetal liver monocytes give rise to self-renewing cells with AM-like phenotype

The fetal liver contains several myeloid precursors including primitive macrophages (pMΦ) and EMP-derived monocytes[22, 23]. Recently, we and others have shown that the latter are the most potent precursors of AM[24, 25]. To identify and better characterize the AM precursor, we sorted populations of viable F4/80^{lo}CD11b^{int}Ly6C^{+} monocytes and viable F4/80^{hi}CD11b^{lo} pMΦ from the fetal liver of E14.5 C57BL/6 embryos (sFig. 1A) and cultured them with GM-CSF *in vitro* (Fig. 1A). Monocytes grew exponentially, whereas pMΦ disappeared within 2 weeks (sFig. 1B). At day 3 of the monocyte culture, a new population with macrophage characteristics (F4/80^{+}Ly6C^{-} cells) emerged, which quickly predominated and appeared to be homogenous after 9 days in the culture (Fig. 1B). The monocyte-to-macrophage differentiation was paralleled by an increase in cell granularity (SSC) and expression of the surface markers CD11c and Siglec-F (sFig. 1C). Similar phenotypic changes also occur during fetal monocyte to AM differentiation in the lung, as described previously[10, 11], although high expression of

CD11b indicated that cultured cells did not fully complete AM differentiation (sFig. 1D)[11]. Notably, the AM-like phenotype was maintained for at least 4 months of continuous culture (sFig. 1D). From here on, we refer to F4/80^{+}CD11c^{+}CD11b^{+}Siglec-F^{+} cells as CSF2-cultured fetal liver monocytes (CSF2-cFliMo). Similar results were obtained when CSF2-cFLiMo were generated from monocytes isolated from E16.5, E18.5, and E20.5 fetal livers (sFig. 1E). When differentiated CSF2-cFliMo cells were deprived of GM-CSF, their numbers rapidly declined (sFig. 1F, G), although the remaining cells maintained the expression of AM surface markers including CD11c and Siglec-F (sFig. 1H).

TGFβR$^{-/-}$ mice are defective in development of AM[26]. Indeed, we found that addition of TGFβ increased the proliferative capacity and the yield of CSF2-cFLiMo, but did not influence the differentiation to AM-like cells (sFig. 2A, B). Notably, culture with TGFβ in the absence of GM-CSF failed to induce proliferation and resulted in death of FLiMo (sFig. 2B). Moreover, TGFβ did not change the phenotype of CSF2-cFliMo after 2-week culture (sFig. 2C).

These results demonstrate that fetal liver monocytes cultured with GM-CSF *in vitro* give rise to a stable population of cells with AM-like phenotype and GM-CSF-dependent self-renewing capacity.

CSF2-cFLiMo develop into mature and functional AM *in vivo*

To assess whether CSF2-cFLiMo can develop to *bona fide* AM and perform AM function *in vivo*, we transferred congenically marked CSF2-cFLiMo intranasally (i.n.) to newborn *Csf2ra*$^{-/-}$ mice (Fig. 1A), which lack AM[12, 24]. Analysis of the BAL and lung of *Csf2ra*$^{-/-}$ recipients showed efficient engraftment of donor-derived cells that resemble mature CD11c^{hi}Siglec-F^{hi} AM (Fig. 1C and sFig. 3A). The numbers of CSF2-cFLiMo-derived AM rapidly increased within the first 6 weeks after transfer, before reaching a relatively stable population size (Fig. 1D), similar to the kinetics during normal postnatal AM differentiation[10, 11]. While CSF2-cFLiMo were CD11b^{hi}Siglec-F^{lo} before transfer, they down-regulated CD11b and up-regulated CD11c and Siglec-F surface expression upon transfer and expansion *in vivo*, indicating that they completed their differentiation to become cells with a phenotype that is indistinguishable from AM of age-matched WT mice (Fig. 1E). Notably, CSF2-cFLiMo-derived AM were maintained in the lung for at least 1 year after transfer (Fig. 1C, D). Moreover, measurement of protein concentration in the BAL at different time points after transfer showed that CSF2-cFLiMo-AM reconstituted *Csf2ra*$^{-/-}$ mice were completely protected from PAP up to one year (Fig. 1F and sFig. 3B). These results demonstrate that CSF2-cFLiMo develop into mature AM, which appear functionally equivalent to *in situ* differentiated AM.

CSF2-cFLiMo-derived AM can self-renew *in vivo*

AM are maintained locally through self-renewal, and they are largely independent of adult hematopoiesis at steady state[10, 11]. Serial transplantation remains the gold standard for experimental assessment of long-term repopulating and self-renewal capacity of hematopoietic stem cells[27], but similar experiments have not been done for tissue macrophages. To determine the long-term self-renewing capacity of CSF2-cFLiMo-AM, we serially transferred *in vitro* differentiated CSF2-cFLiMo or *ex vivo* isolated AM from adult WT mice into neonatal *Csf2ra*$^{-/-}$ mice. After 6 weeks, donor-derived AM were isolated and transferred into a second group of neonatal *Csf2ra*$^{-/-}$ recipients (Fig. 2A). Following secondary transfer, CSF2-cFLiMo-AM and *ex vivo* AM-derived AM (AM-AM) again fully restored the AM compartment of *Csf2ra*$^{-/-}$ recipients and their number and phenotype was comparable to that of AM in the BAL and lung of unmanipulated WT mice (Fig. 2B-D). These results demonstrate that CSF2-cFLiMo-AM have a self-renewal capacity *in vivo*, which is comparable to *bona fide* AM.

CSF2-cFLiMo acquire AM-specific transcriptional signature *in vivo*

To reveal the gene expression programs that are associated with particular AM differentiation stages, we compared the transcriptomes of CSF2-cFLiMo, CSF2-cFLiMo-derived AM to *ex vivo* AM and E14.5 fetal liver monocytes (Fig. 3A). Principal-component analysis (PCA) and matrix clustering, based on all detected genes, revealed that CSF2-cFLiMo-derived AM displayed substantial different gene expression profiles compared to fetal liver monocytes, and CSF2-cFLiMo, while they were closely related and clustered together with *ex vivo* AM (Fig. 3B-C). CSF2-cFLiMo-AM and *ex vivo* AM expressed low levels of several well-known monocyte markers, including *Ly6c1* (Ly-6C), *Fcgr1* (CD64), *Itgam* (CD11b) (Fig. 3D). Moreover, the relative mRNA expression of several established AM markers, including *Marco*, *Pparg*, *Itgax* (CD11c), *MerTk*, *Cd14*, *Fcgr2b* (CD32), *Siglec5* (Siglec-F) and *Chil3* (Ym1) was similar between CSF2-cFLiMo-AM and *ex vivo* AM (Fig. 3D).

Next, we compared differentially expressed genes (DEG) (fold change > 2) to signature genes defined for monocytes and lung macrophages[28]. More than 60% of monocyte signature genes were downregulated, while 60% of AM signature genes were upregulated in in fetal liver monocytes cultured with GM-CSF *in vitro* (sFig. 4A), suggesting that these AM signature genes are directly or indirectly regulated by GM-CSF. Interestingly, the remaining 40% AM signature genes were up-regulated in CSF2-cFLiMo upon transfer and maturation *in vivo* (sFig. 4B).

The *in vitro* culture of precursors followed by *in vivo* transfer described here creates a model to study GM-CSF and other niche factors during AM development. Comparison of the CSF2-cFLiMo and fetal liver monocyte transcriptomes revealed 3301 upregulated and 2657 downregulated genes, which were dependent on GM-CSF (Fig. 3E). Similarly, comparing the transcriptomes of CSF2-cFLiMo-AM to CSF2-cFLiMo, we found 2032 genes that were upregulated and 1813 genes that were down-regulated by niche factors (Fig. 3E). The representative genes of the top 100 DEG regulated by CSF2 or niche factors are listed in Fig. 3F. Only a minor fraction of CSF2-upregulated genes was further upregulated (11.9%) or downregulated (20.3%) by niche factors (Fig. 3G). Similarly, 7.8% and 8.8% of CSF2-downregulated genes were further downregulated or upregulated by niche factors, respectively (Fig. 3G). These results showed that the majority of genes were separately regulated by CSF2 and additional niche factors. More than 60% of the gene expression changes were driven by CSF2 (Fig. 3G), indicating its major contribution to AM development.

Taken together, our results show that culture of fetal liver monocytes with GM-CSF *in vitro* results in AM-like precursors, which can accomplish full AM differentiation driven by alveolar niche factors upon intranasal transfer to AM-deficient neonates.

CSF2-cFLiMo-derived AM are functional in homeostasis and during infection

Overall, our studies demonstrate that CSF2-cFLiMo-AM were functionally equivalent to naturally differentiated AM. To determine the number of donor cells required to fully reconstitute the AM compartment of *Csf2ra*$^{-/-}$ mice, we titrated the number of transferred CSF2-cFLiMo (Fig. 4A). Transfer of a minimum of 5×10^4 CSF2-cFLiMo to neonatal *Csf2ra*$^{-/-}$ mice resulted in AM numbers in adult recipients that were comparable to unmanipulated WT mice (around 5×10^5) (Fig. 4B) and protected mice from PAP (Fig. 4C). We have previously established that around 10% of primary fetal liver monocytes supplied intranasally reach the lung[24]. Thus, CSF2-cFLiMo have expanded around 100-fold 6 weeks after transfer to *Csf2ra*$^{-/-}$ neonates. Notably, extended time of CSF2-cFLiMo *in vitro* culture (i.e. 4 months) prior transfer into recipient mice did not negatively affect their differentiation and functional capacity (Fig. 4B, C). Another critical function of tissue-resident macrophages including AM is the removal of apoptotic cells (efferocytosis)[29]. We compared efferocytosis between CSF2-cFLiMo-AM in *Csf2ra*$^{-/-}$ mice and AM in WT mice by intratracheal (i.t.) installation of labelled apoptotic thymocytes. CSF2-cFLiMo-AM and AM were equally potent at phagocytosing apoptotic cells from the bronchoalveolar space (Fig. 4D).

Next, we assessed whether CSF2-cFLiMo show therapeutic activity upon transfer into adult *Csf2ra*$^{-/-}$ mice, which had already developed PAP. Adult *Csf2ra*$^{-/-}$ mice were transferred i.t. with 0.5, 1 or 2 million CSF2-cFLiMo (Fig. 4E-G). Ten weeks after transfer, donor-derived AM were detectable in the BAL and lung of *Csf2ra*$^{-/-}$ only in recipients transferred with 2 million cells (Fig. 4F). The protein levels in the BAL from mice transferred with 2×10^6 cells were significantly lower when compared to naïve *Csf2ra*$^{-/-}$ mice, suggesting that transferred cells were able to reduce proteinosis, although not to the level of WT mice (Fig. 4G). However, CSF2-cFLiMo-derived AM exhibited higher expression of F4/80 and CD11b, and lower expression of Siglec-F and CD64 when compared to WT AM (sFig. 5A, B), indicating that the AM phenotype was not fully recapitulated but intermediate between AM-derived from CSF2-cFLiMo transferred to neonates and AM-derived from CSF2-cFLiMo transplanted to adult mice. These results show that CSF2-cFLiMo can reproduce AM phenotype and function most adequately only when transferred to neonatal *Csf2ra*$^{-/-}$ mice.

In addition to the homeostatic function, AM play an essential role in protecting influenza virus-infected mice from morbidity by maintaining lung integrity through the removal of dead cells and excess surfactant[11]. To assess the functional capacity of CSF2-cFLiMo-derived AM during pulmonary virus infection, we reconstituted *Csf2ra*$^{-/-}$ neonates with CSF2-cFLiMo and infected adults 10 weeks later with influenza virus PR8 (Fig. 5A). Without transfer, *Csf2ra*$^{-/-}$ mice succumbed to infection due to lung failure (Fig. 5B-E), as reported previously[12]. Notably, the presence of CSF2-cFLiMo-derived-AM protected *Csf2ra*$^{-/-}$ mice from severe morbidity (Fig. 5B, C) and completely restored viability (Fig. 5D) and O_2 saturation (Fig. 5E) compared to infected WT mice.

Recent studies have shown that transplantation of BMM could decrease proteinosis in adult *Csf2rb*$^{-/-}$ mice in homeostasis[18, 19, 30]. To directly compare the capacity of BMM and CSF2-cFLiMo in AM development, we transferred them at a 1:1 ratio into neonatal *Csf2ra*$^{-/-}$ recipient mice (Fig. 5G). Analysis AM compartment 10 weeks after transfer showed that more than 70% were derived from CSF2-cFLiMo (Fig. 4H, I) and that their phenotype (CD11b^{lo}Siglec-F^{hi}) closely resembled that from genuine AM, while the remaining 30% BMM-derived AM showed differences in CD11b, Siglec-F, and CD64 surface levels (Fig. 4J, K). However, transfer of BMM to *Csf2ra*$^{-/-}$ neonates in the absence of competing CSF2-cFLiMo resulted in AM numbers comparable to resident AM in untreated mice (Fig. 5F). To study the function of BMM-derived AM during pulmonary virus infection, we infected *Csf2ra*$^{-/-}$

recipients containing BMM-AM with influenza virus PR8 (Fig. 5A). In contrast to CSF2-cFLiMo-transferred *Csf2ra*$^{-/-}$ mice, the presence of BMM-derived-AM was of no advantage and mice succumbed to infection comparable to *Csf2ra*$^{-/-}$ mice devoid of AM (Fig. 5B-E). These results indicate that CSF2-cFLiMo-derived AM but not BMM-derived AM protect from influenza-induced morbidity and mortality.

Major and minor histocompatibility differences of CSF2-cFLiMo result in transplant rejection

Our results suggest that CSF2-cFLiMo could be used as an elegant *in vitro* and *in vivo* system to study the development and function of AM. To gain more information about the potential of this system, we next evaluated the MHC compatibility in an allogeneic CSF2-cFLiMo transfer. We generated CSF2-cFLiMo from BALB/c E14.5 embryos and transferred them alone, or together with C57BL/6 (B6) CSF2-cFLiMo at a 1:1 ratio into neonatal *Csf2ra*$^{-/-}$ mice that were on B6 background (Fig. 6A). Ten weeks later, we were unable to detect any BALB/c CSF2-cFLiMo-AM, regardless if they had been transferred alone or together with B6 CSF2-cFLiMo, indicating that complete rejection of MHC-mismatched cells (Fig. 6B, C and sFig. 6A, B). We then also compared Y chromosome compatibility by transferring GM-CSF-differentiated monocytes isolated from male neonatal (day 0-3 after birth) liver (CSF2-cNLiMo) to newborn *Csf2ra*$^{-/-}$ male or female recipients (Fig. 6D). Donor-derived AM could be detected in all transferred animals regardless of recipient's sex (Fig. 6E, F). However, female recipients displayed significantly lower AM numbers compared to male recipients, which indicates that there was only a minor Y chromosome-dependent selection. Together, our data indicate that both major histocompatibility complex and minor histocompatibility antigens have to be considered to avoid rejection of AM grafts.

Gene therapy of *Csf2ra* mutant CSF2-cFLiMo

The reconstitution of AM by transferring cultivatable precursors provides unique opportunities for genetic manipulation. To provide proof-of-concept, fetal liver monocytes were purified from E14.5 *Csf2ra*$^{-/-}$ or WT embryos and transduced with a retrovirus encoding *Csf2ra-gfp* (RV$^{Csf2ra\text{-}gfp}$) or control *gfp* only (RV^{gfp}) (Fig. 7A). RV$^{Csf2ra\text{-}gfp}$ transduced *Csf2ra*-deficient FLiMo expanded in the presence of GM-CSF *in vitro* (Fig. 7B) and outgrew all non-transduced cells, as indicated by the presence of almost 100% GFP^{+} cells by day 7 of culture (Fig. 7B, C). As expected, *Csf2ra*-deficient FLiMo transduced with control RV^{gfp} could not expand in culture (Fig. 7B, C). Notably, overexpression of *Csf2ra* in WT FLiMo provided also a slight

growth advantage over non-transduced WT FLiMo *in vitro* (Fig. 7B, C). Next, we transferred RV$^{Csf2ra\text{-}gfp}$ transduced *Csf2ra*-deficient cFLiMo into neonatal *Csf2ra*$^{-/-}$ mice and analyzed BAL and lung 8 weeks later. Indeed, CSF2RA gene therapy of *Csf2ra*-deficient cFLiMo enabled full reconstitution of a functional AM compartment that prevented development of PAP in *Csf2ra*$^{-/-}$ mice (Fig. 7D-G). Transfer of *Csf2ra*-overexpressing WT cFLiMo did not result in higher AM numbers indicating that GM-CSF bioavailability rather than receptor expression is the limiting factor. RV$^{Csf2ra\text{-}gfp}$ transduced cFLiMo-derived AM were phenotypically indistinguishable from unmanipulated WT AM for multiple surface markers, including F4/80, CD11b, CD11c, Siglec-F, and MHCII (Fig 7H). These results provide a proof-of-concept that gene-modified CSF2-cFLiMo differentiate into functional *bona fide* AM, therefore allowing genetic manipulation of this important tissue macrophage compartment.

Discussion

This study describes a two-step AM differentiation model, in which a homogenous, stable immature AM-like population (CSF2-cFLiMo) generated from murine fetal liver monocytes *in vitro*, could efficiently colonize the empty niches and complete differentiation to *bona fide* AM upon transfer to an AM-deficient individual *in vivo*. These CSF2-cFLiMo-AM resemble natural AM phenotypically, transcriptionally, and functionally, and are amenable to genetic modifications. We propose that this AM manipulation system, which integrates ontogeny and tissue imprinting yielding *bona fide* AM, could serve as a potent tool to study AM biology, as well as opening possibilities for therapeutic approaches.

Previous studies have shown that GM-CSF and TGFβ are essential for AM development mainly by induction PPARγ-driven transcriptional program [10, 11, 26]. Our data from FLiMo *in vitro* cultures implicate that GM-CSF is required for AM differentiation, while TGFβ promotes the proliferation of AM/AM precursors. Notably, while GM-CSF induces a transcriptional program by upregulation of PPARγ, which is essential for AM development[10, 11]. Even though FLiMo upregulated a large panel of AM signature genes in the presence of GM-CSF *in vitro*, PCA analysis of the transcriptome showed a difference to that of mature AM. However, upon transfer to the lung, CSF2-cFLiMo completed differentiation into *bona fide* AM indicating that lung tissue instructs terminal differentiation of AM. Thus, our two-step model allows us to separate the transcriptional regulation induced by GM-CSF from other niche factors provided

by lung microenvironment during AM development. Further studies using this model would help to understand transcriptional regulation during AM development.

We showed that low numbers of CSF2-cFLiMo completely restored AM pool of Csf2ra-/- mice within 6 weeks, indicating that they efficiently occupied empty AM niches, and that CSF2-cFLiMo-derived AM possess a long-term self-renewing capacity, as demonstrated by serial transplantation. While this is the gold standard assay for proof of long-term repopulation and self-renewal capacity of hematopoietic stem cells, but to date it has not been used for tissue macrophages according to our knowledge. CSF2-cFLiMo-derived AM prevented PAP, removed apoptotic cells, and protected from fatal influenza infection, indicating that they acquired the broad functional spectrum of bona fide AM.

M-CSF-derived BMM are widely used to study macrophage biology *in vitro*. However, these cells have a limited lifespan and represent only a subset of the macrophage population. They poorly recapitulate features of any tissue-resident macrophage subsets. Another primary macrophage population used as an *in vitro* macrophage model are induced-pluripotent-stem-cell (iPSC)-derived macrophages (iMac), which are genetically and functionally similar to yolk sac[25]-derived primitive macrophages[21, 31]. AM develop from fetal monocytes and are independent of either YS primitive macrophages or bone marrow precursors during homeostasis[8, 22]. Several studies showed recently that AM derived from primitive macrophages or from bone marrow monocytes show differences in metabolism and function[32, 33, 34, 35]. In fact, in this study comparing AM derived from CSF2-cFLiMo or BMM, we found that the latter possess impaired capacity to expand *in vivo* and to acquire a *bona fide* AM phenotype and function, including protection of *Csf2ra*$^{-/-}$ mice from mortality and respiratory failure during influenza infection. Despite being able to reduce proteinosis when transferred in adult *Csf2ra*$^{-/-}$ lung, BMM did not engraft as efficiently in adult lungs as CSF2-cFLiMo-AM. Thus, we propose that CSF2-cFLiMo are differentiated from *bona fide* AM progenitors and represent the most suitable cellular source of AM.

We show that CSF2-cFLiMo transplantation is more efficient in neonates than in adults. CSF2-cFLiMo transferred into neonatal lung expanded and gave rise to *bona fide* AM, while when transplanted into adult lung, they could not efficiently expand and upregulate Siglec-F, CD64 and downregulate CD11b. There are two possible reasons. Firstly, the occurrence of proteinosis in adult *Csf2ra*$^{-/-}$ mice might obstruct the contact between transplanted cells and lung epithelial cells, which is important for the survival and engraftment of transplanted cells. Secondly, the neonatal lung niche could more efficiently promote AM maturation compared to the adult lung niche. So, the macrophage transplantation treatment for hereditary PAP patients

would be more efficient during the neonatal or childhood stage before the occurrence of severe proteinosis. Importantly, we showed that the lung alveolus is not an immune privileged site implicating that transplantation AM-like precursors to MHC- and ever gender-mismatched recipients results in rejection. Thus, our data indicate that both MHC and Y chromosome compatibility require consideration when transferring CSF2-cFLiMo precursors.

CSF2-cFLiMo generated from WT or gene-deficient mice could be used as a high-throughput screening system to study AM development *in vitro* and *in vivo*. Our model is suitable to study the relationship between AM and lung tissue, as well as the roles of specific genes or factors in AM development and function. Furthermore, CSF2-cFLiMo could help to overcome the number limitation of primary macrophages and be used as a therapeutic approach for PAP disease or in other macrophage-based cell therapies for lung emphysema[36], lung fibrosis, lung infectious disease and lung cancer[37, 38]. Finally, genetically modified and transferred CSF2-cFLiMo might facilitate the controlled expression of specific therapeutic proteins in the lung for disease treatment, and therefore, could represent an attractive alternative to non-specific gene delivery by viral vectors.

Methods

Mice

C57BL/6 CD45.2, congenic CD45.1 and, BALB/c mice were originally from the Jackson Laboratory (Bar Harbor, Maine, USA). *Csf2ra*$^{-/-}$ mice were established in our laboratory[12]. All mice were housed and bred under specific pathogen-free conditions in individually ventilated cages in a controlled day-night cycle at the ETH Phenomics Facility. Mice used for experiments were 6-10 weeks (adults) of age, unless otherwise stated. All animal experiments were performed according to the guidelines (Swiss Animal Protection Ordinance (TschV) Zurich) and Swiss animal protection law (TschG) and had been approved by the local animal ethics committee (Kantonales Veterinaersamt Zurich).

Timed pregnancy

Female C57BL/6 CD45.1, CD45.2, or BALB/c mice were housed together with matching male mice overnight. The vaginal plug was checked on the next day and was designated as embryonic day 0.5 (E0.5).

Pulmonary cell transplantation

Neonatal (day 0-3 after birth) *Csf2ra*$^{-/-}$ recipient mice were transferred intranasally (i.n.) with different numbers of cells in 10 μL endotoxin-free PBS. For competitive transfer experiments, 25,000 cells from each origin were mixed and transferred. Adult *Csf2ra*$^{-/-}$ recipient mice were transferred intratracheally (i.t.) with different numbers of cells in 50 μL endotoxin-free PBS.

Cell suspension preparation

Mice were euthanized by overdose (400 mg/kg body weight) of sodium pentobarbital by i.p. injection. The lungs were washed three times with 0.4 ml of ice-cold PBS containing 2 mM EDTA through an intratracheal cannula only when mice were older than 4 weeks. BAL fluid was collected and cells were harvested by centrifugation. Lungs were removed after perfusion with ice-cold PBS. Pregnant females were sacrificed by CO_2 asphyxiation. Fetal livers were removed at the indicated time points. Organs were minced and then digested at 37 °C in IMDM medium containing 2.0 mg/ml of type IV collagenase (Worthington), 0.125 mg/ml DNase I (Sigma) and 3% FCS for 45 min (lungs) or 15 min (fetal and neonatal livers) respectively, and subsequently passed through a 70-μm-cell strainer (Becton Dickinson). Ammonium-chloride-potassium (ACK) lysing buffer was used for erythrocyte lysis for all samples.

Flow cytometry and cell sorting

Multiparameter assessment and cell sorting were performed using LSR Fortessa, BD FACS ARIA II and ARIA III (BD Biosciences) and data were analyzed with FlowJo software (TreeStar). After blocking the FcgIII/II receptors by incubation with homemade anti-CD16/32 (2.4G2), single-cell suspensions were incubated with the indicated fluorochrome-conjugated or biotinylated monoclonal antibodies in FACS buffer (PBS containing 2% FCS and 2 mM EDTA) and then washed twice before detection. Monoclonal antibodies specific to mouse CD45 (30-F11), CD11c (N418), F4/80 (BM8), CD11b (M1/70), Siglec-F (E50-2440, BD Biosciences), CD45.1 (A20), CD45.2 (104), Ly6C (HK1.4), GM-CSFRa (698423, R&D), CD64 (X54-5/7.1) and MHC class II (M5/114.15.2, eBioscience) were purchased from BioLegend unless otherwise stated. Dead cells were excluded using the live/dead marker eFluor780 (eBioscience).

Generation of CSF2-cFLiMo

Fetal livers were harvested from CD45.1^{+} C57BL/6 embryos. Liver single-cell suspensions were prepared. Monocytes were sorted using flow cytometry. Sorted monocytes were cultured

in complete RPMI, supplemented with GM-CSF (PeproTech) (30 ng/mL) *in vitro*. Cells were plated with $1x10^5$ cells/ml and sub-cultured by splitting them 1:5 every 3 days. CSF2-cFLiMo used for transplantation were cultured for 2 weeks in culture media prior to transfers unless stated otherwise.

Generation of BMM

For the preparation of mouse BM-derived macrophages (BMM), tibias and femurs from the hind legs of adult donor mice were flushed with PBS. Bone marrow was rinsed through a 70-um cell strainer (Becton Dickinson) followed by red blood cell depletion with ammonium-chloride-potassium (ACK) lysing buffer. BMM were differentiated *in vitro* in complete RPMI, supplemented with 10 ng/ml M-CSF (PeproTech). Medium was replaced on day 3 and day 6. Adherent cells were harvested and used as mature BMM on day 7 or 8.

Assessment of total protein

Total protein concentrations in BAL fluid were detected by Pierce BCA Protein Assay Kit according to the manufacturer's instructions (Thermo Scientific).

RNA sequencing

100,000 cells of indicated populations were collected into TRIzol (Life Technologies). Phase separation was achieved with the addition of chloroform (Sigma), and total RNA was precipitated from the aqueous layer with isopropanol (Sigma) using glycogen (Roche) as a carrier. RNA samples were sent to the Functional Genomics Center Zurich, where the RNA sequencing was performed. The TruSeq RNA Stranded sample kit (Illumina) was used to construct the sequencing libraries. In brief, total RNA samples (100 ng) were poly (A) enriched and reverse-transcribed into double-stranded cDNA, and TruSeq adapters were then ligated to double-stranded cDNA, then fragments containing TruSeq adapters on both ends were selectively enriched with PCR and subsequently sequenced on the Illumina Nova Seq. The fragments were mapped to the ensemble mouse reference genome GRCm38 (Version25.06.2015) using the STAR aligner[39]. For normalization, the read counts were scaled with the use of the trimmed mean of M-values (TMM) method proposed by Robinson and Oshlack[40]. Principal-component analysis, matrix clustering and heatmap were generated using R.

Efferocytosis of apoptotic cells

Thymocytes were isolated from mice and apoptosis was induced by exposure to 60 mJ/cm^2 UV radiation (Spectrolinker XL-1500; Spectronics Corporation). After 2 h incubation at 37 °C in IMDM + 10% FCS, cells were labeled with 5 mM eFluor670 (eBioscience) according to the manufacturer's instructions, washed extensively with IMDM + 10% FCS and PBS. Then apoptotic cells (5 million cells in 50 μL PBS) were delivered i.t. to recipient mice. 0.5, 2 and 22 h after administration, efferocytosis by AM in the BAL and lung was assessed by flow cytometry.

Influenza viral infection

Influenza virus strain PR8 (A/Puerto Rico/34, H1N1) was originally provided by J. Pavlovic, University Zurich. For infections, the mice were anesthetized and intratracheally (i.t.) inoculated with indicated doses of virus in 50 ul endotoxin-free PBS. Temperature and weight of mice were monitored daily and animals were euthanized if they fulfilled the severity criteria set out by institutional and cantonal guidelines.

Measurement of oxygen saturation

The MouseOx^{TM} Puls-oximeter (Starr Life Sciences) was used to measure oxygen (O_2) saturation in influenza-infected mice on day 7 post infection. The depilatory agent was applied to the neck of mice 2-3 days prior to measurement to remove hair. Mice were sedated with 2.5mg/kg intraperitoneal Midazolam (Roche) 0.5-1 hour before measurement. The sensor clip was placed on the neck and O_2 saturation was measured each second over 3-5 min per mouse. Data shown is the average value of each mouse.

RV-reconstitution of CSF2RA gene

Two retroviral constructs based on moloney murine leukemia virus, containing Csf2ra cDNA and GFP (RV$^{Csf2ra\text{-}gfp}$) or GFP only (RV^{gfp}), were used for transfection of retrovirus packaging cell line. Fresh viral supernatants containing non-replicating retroviruses were used for transduction of fetal liver monocytes isolated as described above from *Csf2ra*$^{-/-}$ or CD45.1^{+} WT embryos. Cells were cultured in complete RPMI, supplemented with GM-CSF (30 ng/mL) for 7 days. All non-transduced fetal liver monocytes derived from *Csf2ra*$^{-/-}$ embryos could not proliferate. After a week, a homogenous population of receptor-expressing cells was detected and used for transfers. For WT cells, all live cells treated with the Csf2ra-overexpressing virus were used (irrespectively of the transduction level).

Statistical analysis

Mean values and SEM were calculated with Prism (GraphPad Software, Inc). Student's t-test (unpaired) was used for comparing two groups, and ANOVA (one way) was used for comparing multiple groups: ns, not significant; *$p < 0.05$, **$p < 0.01$, ***$p < 0.001$, ****$p < 0.0001$.

Acknowledgements

We thank the teams of the ETH Flow Cytometry Core Facility for cell sorting and the EPIC mouse facility for animal husbandry, Peter Nielsen for discussion and editing of the manuscript. We are grateful for research grants from SNF (310030_163443 and 310030B_182829).

Author contributions

F.L., K.O., and M.K. designed the experiments; F.L. and K.O. performed and analyzed the experiments. L.P. analyzed RNA sequencing data. C.S. and M.K. discussed data and provided conceptualization. F.L., K.O., and M.K. wrote the manuscript.

References

1. Davies, L.C., Jenkins, S.J., Allen, J.E. & Taylor, P.R. Tissue-resident macrophages. *Nat Immunol* **14**, 986-995 (2013).

2. Hoeffel, G. & Ginhoux, F. Ontogeny of Tissue-Resident Macrophages. *Front Immunol* **6**, 486 (2015).

3. Moroni, F. *et al.* Safety profile of autologous macrophage therapy for liver cirrhosis. *Nat Med* **25**, 1560-1565 (2019).

4. Duan, Z. & Luo, Y. Targeting macrophages in cancer immunotherapy. *Signal Transduct Target Ther* **6**, 127 (2021).

5. Peng, R. *et al.* Macrophage-Based Therapies for Atherosclerosis Management. *J Immunol Res* **2020**, 8131754 (2020).

6. Hussell, T. & Bell, T.J. Alveolar macrophages: plasticity in a tissue-specific context. *Nat Rev Immunol* **14**, 81-93 (2014).

7. Kopf, M., Schneider, C. & Nobs, S.P. The development and function of lung-resident macrophages and dendritic cells. *Nat Immunol* **16**, 36-44 (2015).

8. Yona, S. *et al.* Fate mapping reveals origins and dynamics of monocytes and tissue macrophages under homeostasis. *Immunity* **38**, 79-91 (2013).

9. Hashimoto, D. *et al.* Tissue-resident macrophages self-maintain locally throughout adult life with minimal contribution from circulating monocytes. *Immunity* **38**, 792-804 (2013).

10. Guilliams, M. *et al.* Alveolar macrophages develop from fetal monocytes that differentiate into long-lived cells in the first week of life via GM-CSF. *J Exp Med* **210**, 1977-1992 (2013).

11. Schneider, C. *et al.* Induction of the nuclear receptor PPAR-gamma by the cytokine GM-CSF is critical for the differentiation of fetal monocytes into alveolar macrophages. *Nat Immunol* **15**, 1026-1037 (2014).

12. Schneider, C. *et al.* Frontline Science: Coincidental null mutation of Csf2ralpha in a colony of PI3Kgamma-/- mice causes alveolar macrophage deficiency and fatal respiratory viral infection. *J Leukoc Biol* **101**, 367-376 (2017).

13. Robb, L. *et al.* Hematopoietic and lung abnormalities in mice with a null mutation of the common beta subunit of the receptors for granulocyte-macrophage colony-stimulating factor and interleukins 3 and 5. *Proc Natl Acad Sci U S A* **92**, 9565-9569 (1995).

14. Nishinakamura, R. *et al.* Mice deficient for the IL-3/GM-CSF/IL-5 beta c receptor exhibit lung pathology and impaired immune response, while beta IL3 receptor-deficient mice are normal. *Immunity* **2**, 211-222 (1995).

15. Suzuki, T. *et al.* Hereditary pulmonary alveolar proteinosis caused by recessive CSF2RB mutations. *Eur Respir J* **37**, 201-204 (2011).

16. Suzuki, T. *et al.* Familial pulmonary alveolar proteinosis caused by mutations in CSF2RA. *J Exp Med* **205**, 2703-2710 (2008).

17. Trapnell, B.C., Whitsett, J.A. & Nakata, K. Pulmonary alveolar proteinosis. *N Engl J Med* **349**, 2527-2539 (2003).

18. Happle, C. *et al.* Pulmonary transplantation of macrophage progenitors as effective and long-lasting therapy for hereditary pulmonary alveolar proteinosis. *Sci Transl Med* **6**, 250ra113 (2014).

19. Suzuki, T. *et al.* Pulmonary macrophage transplantation therapy. *Nature* **514**, 450-454 (2014).

20. Mucci, A. *et al.* iPSC-Derived Macrophages Effectively Treat Pulmonary Alveolar Proteinosis in Csf2rb-Deficient Mice. *Stem Cell Reports* **11**, 696-710 (2018).

21. Takata, K. *et al.* Induced-Pluripotent-Stem-Cell-Derived Primitive Macrophages Provide a Platform for Modeling Tissue-Resident Macrophage Differentiation and Function. *Immunity* **47**, 183-198 e186 (2017).

22. Hoeffel, G. *et al.* C-Myb(+) erythro-myeloid progenitor-derived fetal monocytes give rise to adult tissue-resident macrophages. *Immunity* **42**, 665-678 (2015).

23. Gomez Perdiguero, E. *et al.* Tissue-resident macrophages originate from yolk-sac-derived erythro-myeloid progenitors. *Nature* **518**, 547-551 (2015).

24. Li, F., Okreglicka, K.M., Pohlmeier, L.M., Schneider, C. & Kopf, M. Fetal monocytes possess increased metabolic capacity and replace primitive macrophages in tissue macrophage development. *EMBO J* **39**, e103205 (2020).

25. van de Laar, L. *et al.* Yolk Sac Macrophages, Fetal Liver, and Adult Monocytes Can Colonize an Empty Niche and Develop into Functional Tissue-Resident Macrophages. *Immunity* **44**, 755-768 (2016).

26. Yu, X. *et al.* The Cytokine TGF-beta Promotes the Development and Homeostasis of Alveolar Macrophages. *Immunity* **47**, 903-912 e904 (2017).

27. Iscove, N.N. & Nawa, K. Hematopoietic stem cells expand during serial transplantation in vivo without apparent exhaustion. *Curr Biol* **7**, 805-808 (1997).

28. Lavin, Y. *et al.* Tissue-resident macrophage enhancer landscapes are shaped by the local microenvironment. *Cell* **159**, 1312-1326 (2014).

29. Morioka, S., Maueroder, C. & Ravichandran, K.S. Living on the Edge: Efferocytosis at the Interface of Homeostasis and Pathology. *Immunity* **50**, 1149-1162 (2019).

30. Lachmann, N. *et al.* Gene correction of human induced pluripotent stem cells repairs the cellular phenotype in pulmonary alveolar proteinosis. *Am J Respir Crit Care Med* **189**, 167-182 (2014).

31. Buchrieser, J., James, W. & Moore, M.D. Human Induced Pluripotent Stem Cell-Derived Macrophages Share Ontogeny with MYB-Independent Tissue-Resident Macrophages. *Stem Cell Reports* **8**, 334-345 (2017).

32. Machiels, B. *et al.* A gammaherpesvirus provides protection against allergic asthma by inducing the replacement of resident alveolar macrophages with regulatory monocytes. *Nat Immunol* **18**, 1310-1320 (2017).

33. Misharin, A.V. *et al.* Monocyte-derived alveolar macrophages drive lung fibrosis and persist in the lung over the life span. *J Exp Med* **214**, 2387-2404 (2017).

34. Gibbings, S.L. *et al.* Transcriptome analysis highlights the conserved difference between embryonic and postnatal-derived alveolar macrophages. *Blood* **126**, 1357-1366 (2015).

35. Aegerter, H. *et al.* Influenza-induced monocyte-derived alveolar macrophages confer prolonged antibacterial protection. *Nat Immunol* **21**, 145-157 (2020).

36. Wilson, A.A. *et al.* Amelioration of emphysema in mice through lentiviral transduction of long-lived pulmonary alveolar macrophages. *J Clin Invest* **120**, 379-389 (2010).

37. Lee, S., Kivimae, S., Dolor, A. & Szoka, F.C. Macrophage-based cell therapies: The long and winding road. *J Control Release* **240**, 527-540 (2016).

38. Byrne, A.J., Maher, T.M. & Lloyd, C.M. Pulmonary Macrophages: A New Therapeutic Pathway in Fibrosing Lung Disease? *Trends Mol Med* **22**, 303-316 (2016).

39. Dobin, A. *et al.* STAR: ultrafast universal RNA-seq aligner. *Bioinformatics* **29**, 15-21 (2013).

40. Robinson, M.D. & Oshlack, A. A scaling normalization method for differential expression analysis of RNA-seq data. *Genome Biol* **11**, R25 (2010).

Figure Legends

Figure 1. Fetal liver monocytes can proliferate *in vitro* with GM-CSF and further develop into mature functional AM *in vivo*

(A) Illustration of experimental regime. Primary monocytes from fetal liver were cultured *in vitro* with GM-CSF. (B) Representative dot plots for F4/80 vs Ly6C are shown for GM-CSF-cultured fetal liver monocytes (CSF2-cFLiMo) at the indicated time points, pre-gated on viable $CD45^+$ single cells. (C-F) 5×10^4 CSF2-cFLiMo generated from CD45.1 E14.5 embryos, after 2 weeks of culturing, were transferred intranasally (i.n.) to neonatal (day 0-3 after birth) $CD45.2^+$ *Csf2ra*$^{-/-}$ mice and analyzed at the indicated time points. (C) Representative dot plots of donor-derived cells in the bronchoalveolar lavage (BAL) of recipients 6 weeks, 6 months and 1 year after transfer, pre-gated as viable single cells. (D) Total numbers of donor-derived AM from lung (1 and 2 weeks) or from BAL and lung (after 6 weeks) detected in recipients at the indicated time-points. (E) Representative histograms of AM signature marker expression on CSF2-cFLiMo before transfer, CSF2-cFLiMo-derived AM detected in *Csf2ra*$^{-/-}$ recipient mice 6 weeks after transfer, and endogenous AM from age-matched control mice showing FMO control (grey) and specific antibodies against the indicated markers (black line). (F) Total protein in the BAL of CSF2-cFLiMo-transferred *Csf2ra*$^{-/-}$, unmanipulated *Csf2ra*$^{-/-}$ and WT mice. The data are representative of three independent experiments. Values show means ± SEM of three to five mice per group in D and F. Student's t test (unpaired) was used in F: ns, not significant; *$p < 0.05$, **$p < 0.01$, ***$p < 0.001$, ****$p < 0.0001$.

Figure 2. CSF2-cFLiMo-derived AM have ability to self-renew *in vivo*

(A) Illustration of experimental regime. 5×10^4 of CD45.1 CSF2-cFLiMo generated from E14.5 embryos after 2-week culture or CD45.1 AM sorted from WT adult mice were transferred i.n. to neonatal CD45.2 *Csf2ra*$^{-/-}$ mice. After 6 weeks, donor-derived AM were sorted and 5×10^4 of cells were transferred i.n. to new neonatal *Csf2ra*$^{-/-}$ mice. BAL and lung were analysed 6 weeks after second-round transfer in B-D. (B) Representative dot plots showing the phenotype of CD45.1 donor-derived AM in the BAL and lung, pre-gated as viable $CD45^+$ single cells. (C-D) Numbers of donor-derived AM and WT AM in the BAL (C) and lung (D). Age-matched *Csf2ra*$^{-/-}$ and CD45.2 WT mice were included as negative and positive controls, respectively. The data are representative of three experiments. Values show means ± SEM of three to four mice per group. ANOVA (one way) was used in C-D: ns, not significant; *$p < 0.05$, **$p < 0.01$, ***$p < 0.001$, ****$p < 0.0001$.

Figure 3. Gene expression profiles of transferred CSF2-cFLiMo in *Csf2ra*$^{-/-}$ mice

(A) Illustration of experimental regime. Primary monocytes from E14.5 fetal liver were sorted using flow cytometry. CSF2-cFLiMo were collected after 2 weeks. CSF2-cFLiMo were transferred i.n. to neonatal *Csf2ra*$^{-/-}$ mice. Mice were analysed 6 weeks after transfer and CSF2-cFLiMo-derived mature AM (CSF2-cFLiMo-AM) were sorted from the BAL as viable CD45^{+}CD11c^{hi}F4/80^{+}Siglec-F^{hi}CD11b^{lo} cells. AM from 6-week-old WT mice were sorted as control. RNA sequencing was performed (two biological replicates per group). (B) Principal component analysis (PCA) and (C) matrix clustering of the transcriptomes of all samples are shown. (D) Heat maps showing expression of monocyte and AM markers. (E) The numbers of upregulated and downregulated genes by CSF2 or niche. (F) Heat map showing the top 100 DEG and reprehensive genes of CSF2 and niche regulated. (G) Venn diagram of differentially expressed genes. Intersections of CSF2-upregulated or CSF2-downregulated vs niche-upregulated or niche-downregulated genes. The absolute gene numbers and percentages in the intersections are shown.

Figure 4. CSF2-cFLiMo-derived AM are functional in phagocytosis and efferocytosis

(A) Illustration of experimental regime. Different numbers of CD45.1 CSF2-cFLiMo after 2-week (2w) or 4-month (4m) of culturing were transferred i.n to neonatal CD45.2 *Csf2ra*$^{-/-}$ mice and analysed 6 weeks later in B-C. (B) Total numbers of donor-derived AM in the BAL and lung of recipient *Csf2ra*$^{-/-}$ mice or AM in the BAL and lung of WT mice. (C) Total protein levels in the BAL. (D) Efferocytosis of i.t. instilled apoptotic thymocytes by AM at the indicated time points. Values shown depict percentages of efferocytic AM. (E) Illustration of experimental regime. CD45.1 C57/BL6 CSF2-cFLiMo were generated from E14.5 embryos and cultured 2 weeks *in vitro*. Different numbers of CSF2-cFLiMo were transferred i.t. to 10-week-old adult *Csf2ra*$^{-/-}$ mice and analysed 10 weeks later in F-G. (F) Total numbers of donor-derived AM in the BAL and lung of recipient *Csf2ra*$^{-/-}$ mice or AM in the BAL and lung of WT mice. (G) Total protein levels in the BAL. Age-matched *Csf2ra*$^{-/-}$ and WT C57BL/6 mice were included as negative and positive controls, respectively. Values show means ± SEM and the results are representative of three experiments. Student's t test (unpaired) was used in D and ANOVA (one way) was used in B, C, F and G: ns, not significant; *$p < 0.05$, **$p < 0.01$, ***$p < 0.001$, ****$p < 0.0001$.

Figure 5. CSF2-cFLiMo, but not BMM transplantation protects *Csf2ra*$^{-/-}$ mice from respiratory failure following influenza infection.

(A) Illustration of experimental regime. CSF2-cFLiMo generated from E14.5 embryos after 2-week culture or BMM generated from adults after 7-day culture were i.n. transferred to neonatal CD45.2 *Csf2ra*$^{-/-}$ mice. Adult recipient mice were infected i.t. with 10 pfu PR8 influenza virus and analysed in B-F. Shown are loss of body weight (B) and temperature (C), relative to the day of infection. (D) Survival curve showing the fraction of surviving animals for each day after infection. (E) Oxygen (O_2) saturation on 7 days p.i. is shown. (F) Donor-derived AM numbers in the BAL and lung of *Csf2ra*$^{-/-}$ mice 8 weeks after AM reconstitution described in Fig. 5A and prior to infection. Age-matched *Csf2ra*$^{-/-}$ and WT mice were included as negative and positive controls, respectively. (G) Illustration of experimental regime. CD45.1 CSF2-cFLiMo were generated from E14.5 embryos and cultured 2 weeks *in vitro*. CD45.1CD45.2 BMM were generated from adults and cultured 7 days *in vitro*. CSF2-cFLiMo and BMM were pooled in 1:1 ratio and transferred i.n. to neonatal CD45.2 *Csf2ra*$^{-/-}$ mice and analysed 10 weeks later in H-K. (H-I) Representative dot plots (H) and percentage (I) of donor-derived AM in BAL and lung of the recipients. (J-K) Representative histograms (J) and mean fluorescence intensity (MFI) (K) of AM signature markers on CSF2-cFLiMo- and BMM-derived AM and WT AM. Values show means ± SEM and the results are representative of three experiments. Student's t test (unpaired) was used in I and ANOVA (one way) was used in E, F and K: ns, not significant; *$p < 0.05$, **$p < 0.01$, ***$p < 0.001$, ****$p < 0.0001$.

Figure 6. The MHC and gender compatibility in allogenic CSF2-cFLiMo transfers

(A) Illustration of experimental regime. CD45.2 BALB/c and CD45.1 B6 CSF2-cFLiMo were generated from E14.5 embryos and cultured 2 weeks *in vitro*. BALB/c CSF2-cFLiMo were transferred to neonatal CD45.2 *Csf2ra*$^{-/-}$ mice (B6 background) either separately or in a 1:1 ratio with B6 CSF2-cFLiMo and analysed 10 weeks later in B-C. (B) Representative dot plots showing the phenotype of donor-derived AM in the BAL, pre-gated on viable CD45^{+} single cells. (C) Percentage of donor-derived AM in BAL of co-transferred recipients. (D) Illustration of experimental regime. CSF2-cNLiMo generated from CD45.1 WT male neonates after 2-week culture were intranasally transferred to neonatal CD45.2 *Csf2ra*$^{-/-}$ mice respectively and analysed after 10 weeks in E-F. Mice were grouped according to gender. (E-F) Numbers of donor-derived AM and WT AM in the BAL (E) and lung (F) are shown. Age-matched *Csf2ra*$^{-/-}$ and CD45.2 WT mice were included as negative and positive controls in B, E and F. Values show means ± SEM in C, E and F and the results are representative of three experiments.

Student's t test (unpaired) was used: ns, not significant; *p < 0.05, **p < 0.01, ***p < 0.001, ****p < 0.0001.

Figure 7. Csf2ra-reconstituted *Csf2ra*$^{-/-}$ CSF2-cFLiMo can differentiate into functional AM *in vivo*

(A) Illustration of experimental regime. Fetal liver (FL) monocytes were purified from E14.5 CD45.2 *Csf2ra*$^{-/-}$ or CD45.1 WT embryos and spin infected with GM-CSFRa-GFP or GFP (control) retrovirus (RV$^{Csf2ra\text{-}gfp}$ or RV^{gfp}). Cells were cultured with CSF2 for 7 days. RV$^{Csf2ra\text{-}gfp}$ transduced *Csf2ra*$^{-/-}$ CSF2-cFLiMo (RV$^{Csf2ra\text{-}gfp}$-cFLiMo) or identically treated CD45.1 WT CSF2-cFLiMo were transferred i.n. to neonatal CD45.2^{+} *Csf2ra*$^{-/-}$ mice and evaluated after 8 weeks. (B) Efficiency of spin infection (GFP^{+}) and survival of cultured cells at day 3 and 7 post-infection. (C) Expression levels of GM-CSFRa on RV$^{Csf2ra\text{-}gfp}$ or RV^{gfp} transduced *Csf2ra*$^{-/-}$ or WT cFLiMo at day 3 and 7 post-infection. (D) Representative dot plots showing the phenotype of donor-derived cells in the BAL and lung, pre-gated on viable CD45^{+} single cells. (E-F) Numbers of donor-derived AM and WT AM in the BAL (E) and lung (F). (G) Total protein levels in the BAL are shown. Age-matched *Csf2ra*$^{-/-}$ and CD45.2 WT mice were included as negative and positive controls in D-G, respectively. (H) Representative histograms of AM signature marker expression, GM-CSFRa and GFP on RV$^{Csf2ra\text{-}gfp}$-cFLiMo-derived AM and WT AM showing FMO control (grey) and specific antibodies against indicated markers (black line). The data are representative of three experiments. Values show means ± SEM of three to four mice per group. Student's t test (unpaired) was used in E-G: ns, not significant; *p < 0.05, **p < 0.01, ***p < 0.001, ****p < 0.0001.

Figure 1

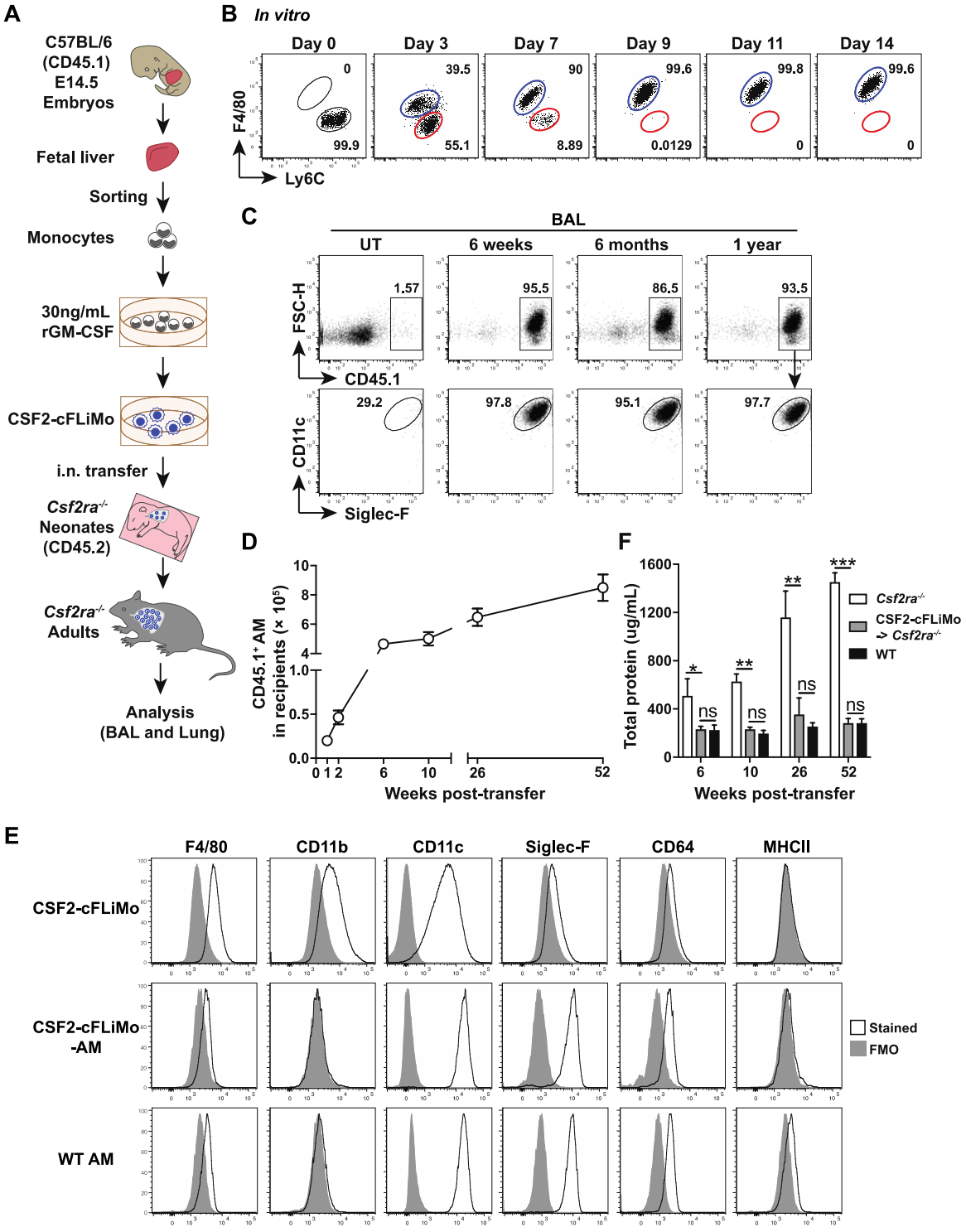
A
C57BL/6 (CD45.1) E14.5 Embryos
Fetal liver
Sorting
Monocytes
30ng/mL rGM-CSF
CSF2-cFLiMo
i.n. transfer
Csf2ra-/- Neonates (CD45.2)
Csf2ra-/- Adults
Analysis (BAL and Lung)
B In vitro
Day 0
Day 3
Day 7
Day 9
Day 11
Day 14
F4/80
Ly6C
0
99.9
39.5
55.1
90
8.89
99.6
0.0129
99.8
0
99.6
0
C
BAL
UT
6 weeks
6 months
1 year
FSC-H
CD45.1
1.57
95.5
86.5
93.5
CD11c
Siglec-F
29.2
97.8
95.1
97.7
D
CD45.1+ AM in recipients (× 10^5)
Weeks post-transfer
F
Total protein (ug/mL)
Weeks post-transfer
Csf2ra-/-
CSF2-cFLiMo -> Csf2ra-/-
WT
ns
E
F4/80
CD11b
CD11c
Siglec-F
CD64
MHCII
CSF2-cFLiMo
CSF2-cFLiMo -AM
WT AM
Stained
FMO

Figure 2

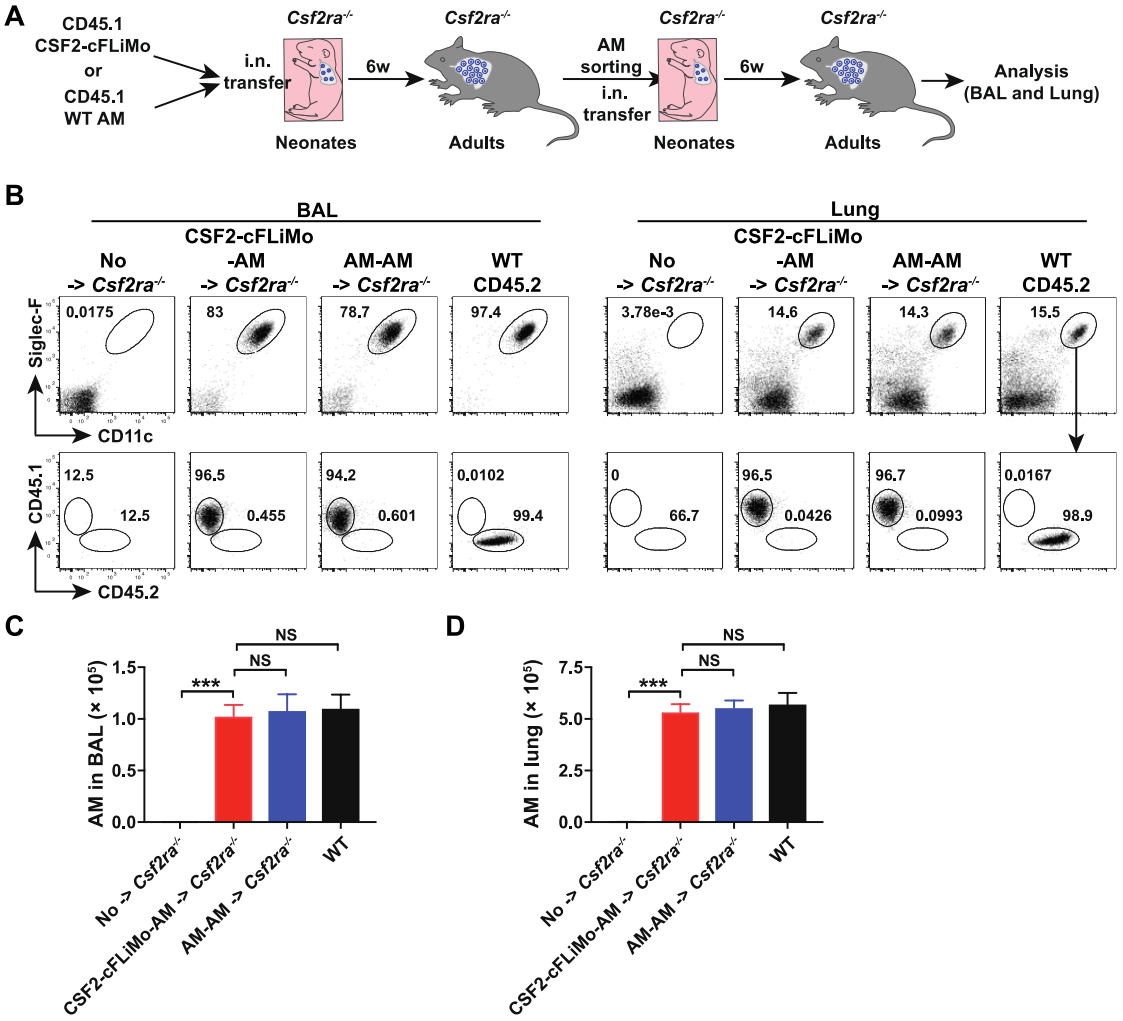
A
CD45.1
CSF2-cFLiMo
or
CD45.1
WT AM
i.n.
transfer
Csf2ra-/-
Neonates
6w
Csf2ra-/-
Adults
AM
sorting
i.n.
transfer
Csf2ra-/-
Neonates
6w
Csf2ra-/-
Adults
Analysis
(BAL and Lung)
B
BAL
Lung
CSF2-cFLiMo
No -> Csf2ra-/-
-AM -> Csf2ra-/-
AM-AM -> Csf2ra-/-
WT CD45.2
Siglec-F
CD11c
CD45.1
CD45.2
0.0175
83
78.7
97.4
3.78e-3
14.6
14.3
15.5
12.5
12.5
96.5
0.455
94.2
0.601
0.0102
99.4
0
66.7
96.5
0.0426
96.7
0.0993
0.0167
98.9
C
AM in BAL (× 10^5)
1.5
1.0
0.5
0.0
***
NS
NS
No -> Csf2ra-/-
CSF2-cFLiMo-AM -> Csf2ra-/-
AM-AM -> Csf2ra-/-
WT
D
AM in lung (× 10^5)
7.5
5.0
2.5
0.0
***
NS
NS
No -> Csf2ra-/-
CSF2-cFLiMo-AM -> Csf2ra-/-
AM-AM -> Csf2ra-/-
WT

Figure 3

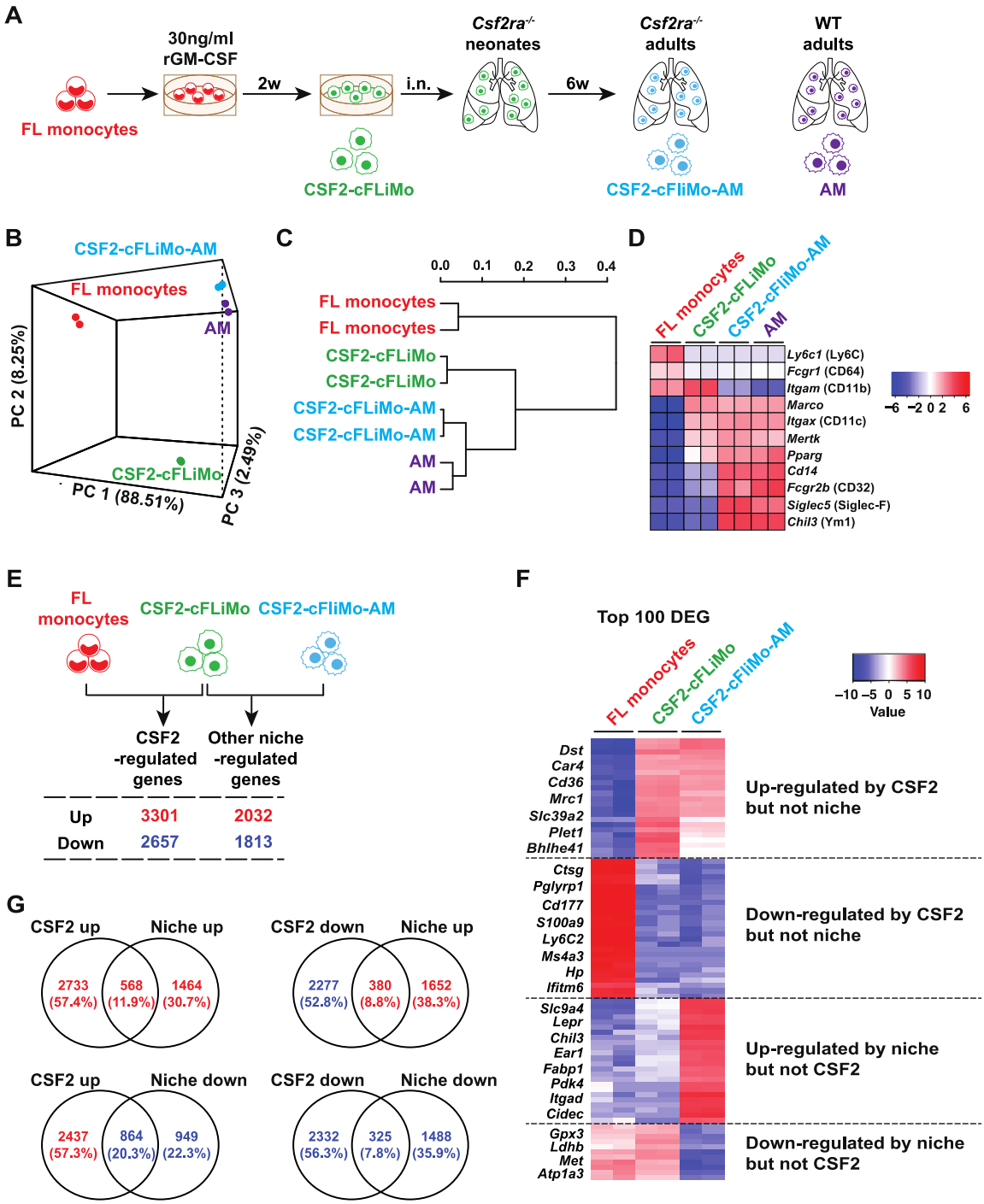
A
30ng/ml
rGM-CSF
2w
i.n.
6w
FL monocytes
CSF2-cFLiMo
Csf2ra-/-
neonates
Csf2ra-/-
adults
WT
adults
CSF2-cFliMo-AM
AM
B
CSF2-cFLiMo-AM
FL monocytes
AM
CSF2-cFLiMo
PC 2 (8.25%)
PC 1 (88.51%)
PC 3 (2.49%)
C
0.0 0.1 0.2 0.3 0.4
FL monocytes
FL monocytes
CSF2-cFLiMo
CSF2-cFLiMo
CSF2-cFLiMo-AM
CSF2-cFLiMo-AM
AM
AM
D
FL monocytes
CSF2-cFLiMo
CSF2-cFliMo-AM
AM
Ly6c1 (Ly6C)
Fcgr1 (CD64)
Itgam (CD11b)
Marco
Itgax (CD11c)
Mertk
Pparg
Cd14
Fcgr2b (CD32)
Siglec5 (Siglec-F)
Chil3 (Ym1)
−6 −2 0 2 6
E
FL monocytes
CSF2-cFLiMo
CSF2-cFliMo-AM
CSF2 -regulated genes
Other niche -regulated genes
Up 3301 2032
Down 2657 1813
F
Top 100 DEG
FL monocytes
CSF2-cFLiMo
CSF2-cFliMo-AM
−10 −5 0 5 10
Value
Dst
Car4
Cd36
Mrc1
Slc39a2
Plet1
Bhlhe41
Up-regulated by CSF2 but not niche
Ctsg
Pglyrp1
Cd177
S100a9
Ly6C2
Ms4a3
Hp
Ifitm6
Down-regulated by CSF2 but not niche
Slc9a4
Lepr
Chil3
Ear1
Fabp1
Pdk4
Itgad
Cidec
Up-regulated by niche but not CSF2
Gpx3
Ldhb
Met
Atp1a3
Down-regulated by niche but not CSF2
G
CSF2 up
Niche up
2733 (57.4%)
568 (11.9%)
1464 (30.7%)
CSF2 down
Niche up
2277 (52.8%)
380 (8.8%)
1652 (38.3%)
CSF2 up
Niche down
2437 (57.3%)
864 (20.3%)
949 (22.3%)
CSF2 down
Niche down
2332 (56.3%)
325 (7.8%)
1488 (35.9%)

Figure 4

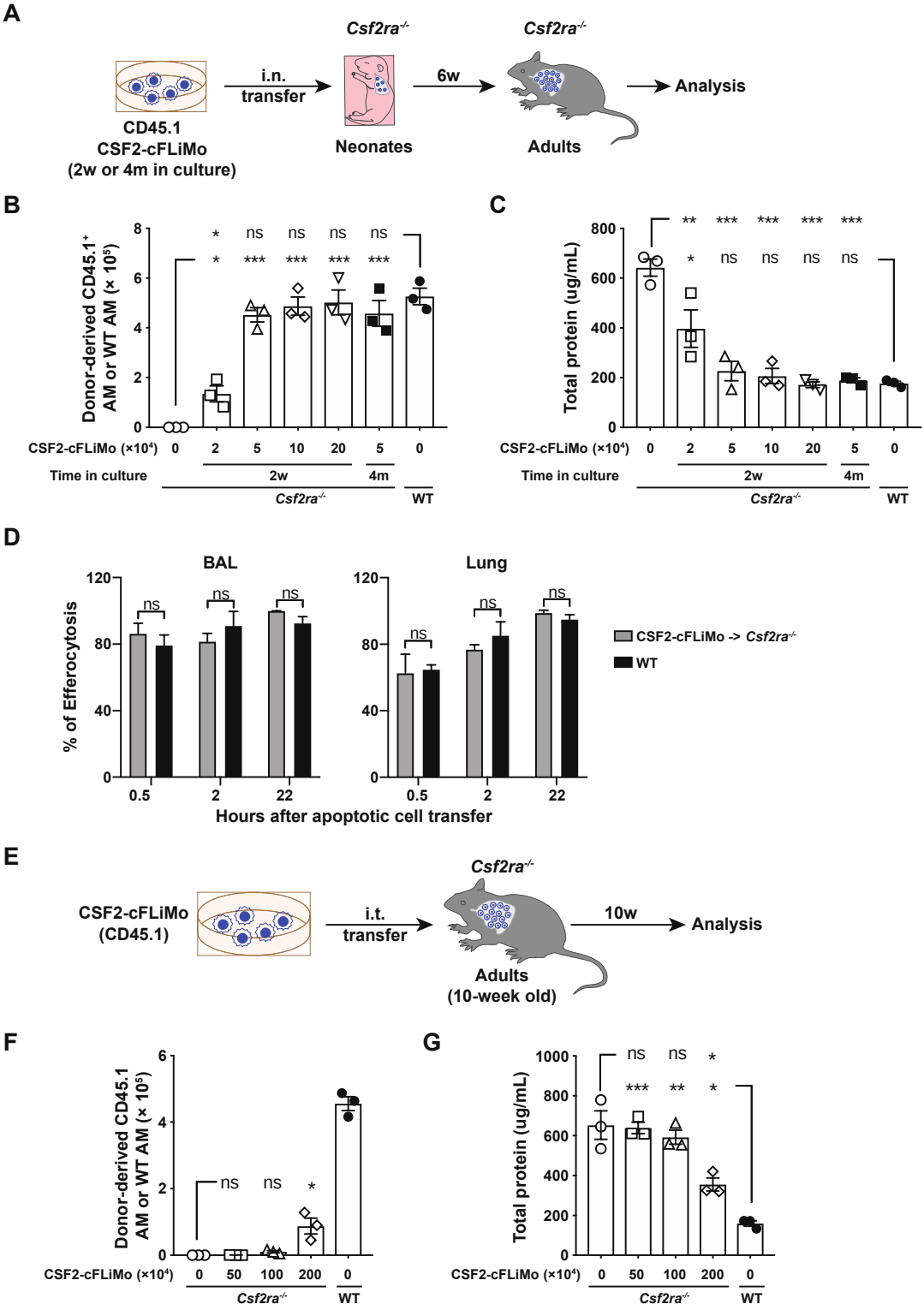
A
Csf2ra-/-
Csf2ra-/-
i.n.
transfer
6w
Analysis
CD45.1
CSF2-cFLiMo
(2w or 4m in culture)
Neonates
Adults
B
Donor-derived CD45.1+ AM or WT AM (× 10^5)
CSF2-cFLiMo (×10^4)
Time in culture
2w
4m
Csf2ra-/-
WT
C
Total protein (ug/mL)
D
BAL
Lung
% of Efferocytosis
Hours after apoptotic cell transfer
CSF2-cFLiMo -> Csf2ra-/-
WT
E
CSF2-cFLiMo
(CD45.1)
i.t.
transfer
10w
Analysis
Adults
(10-week old)
F
G

Figure 5

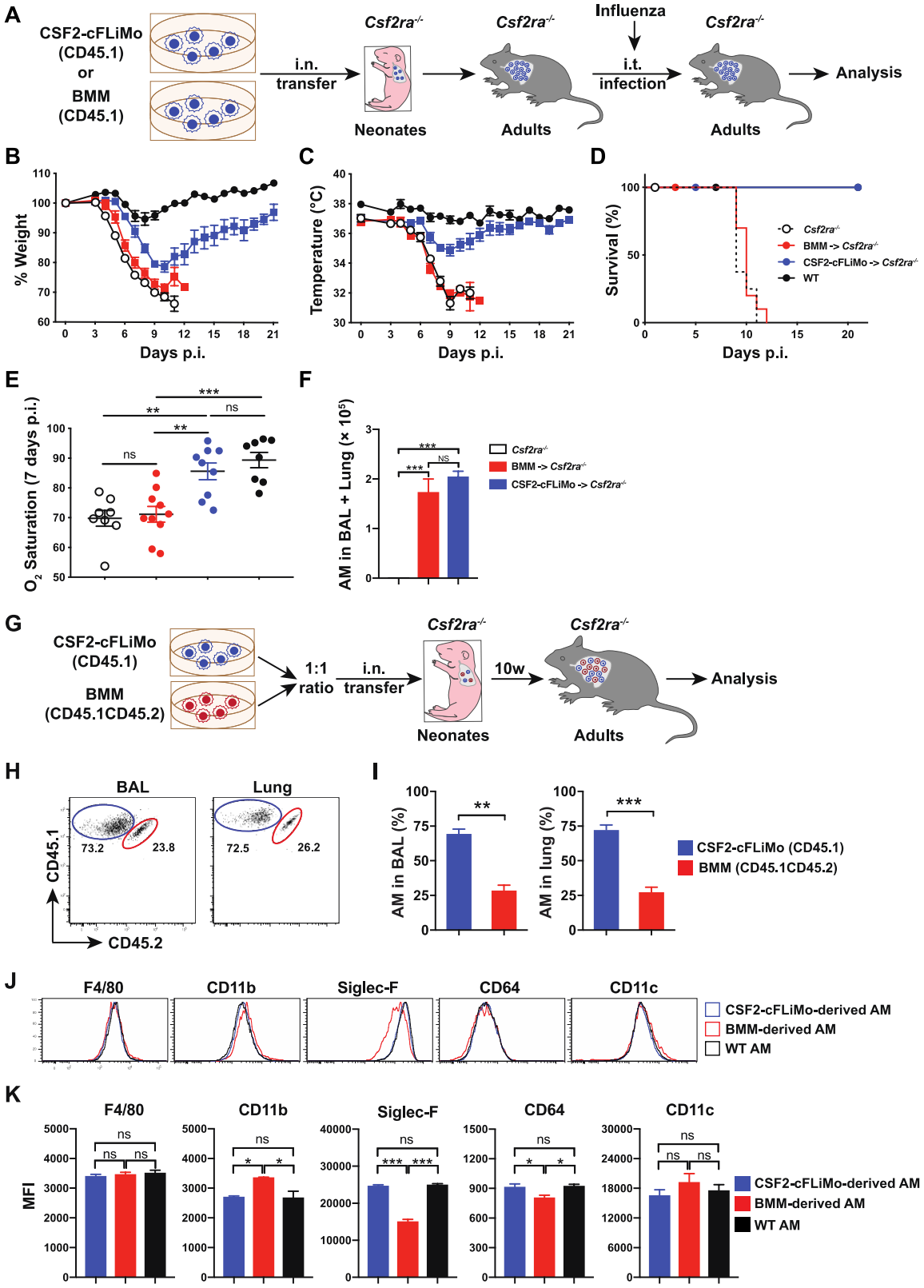
A
CSF2-cFLiMo (CD45.1)
or
BMM (CD45.1)
i.n. transfer
Csf2ra-/-
Neonates
Csf2ra-/-
Adults
Influenza
i.t. infection
Csf2ra-/-
Adults
Analysis
B
% Weight
Days p.i.
C
Temperature (°C)
Days p.i.
D
Survival (%)
Days p.i.
Csf2ra-/-
BMM -> Csf2ra-/-
CSF2-cFLiMo -> Csf2ra-/-
WT
E
O2 Saturation (7 days p.i.)
F
AM in BAL + Lung (× 10^5)
Csf2ra-/-
BMM -> Csf2ra-/-
CSF2-cFLiMo -> Csf2ra-/-
G
CSF2-cFLiMo (CD45.1)
BMM (CD45.1CD45.2)
1:1 ratio
i.n. transfer
Csf2ra-/-
Neonates
10w
Csf2ra-/-
Adults
Analysis
H
BAL
Lung
CD45.1
CD45.2
73.2
23.8
72.5
26.2
I
AM in BAL (%)
AM in lung (%)
CSF2-cFLiMo (CD45.1)
BMM (CD45.1CD45.2)
J
F4/80
CD11b
Siglec-F
CD64
CD11c
CSF2-cFLiMo-derived AM
BMM-derived AM
WT AM
K
MFI
F4/80
CD11b
Siglec-F
CD64
CD11c
CSF2-cFLiMo-derived AM
BMM-derived AM
WT AM

Figure 6

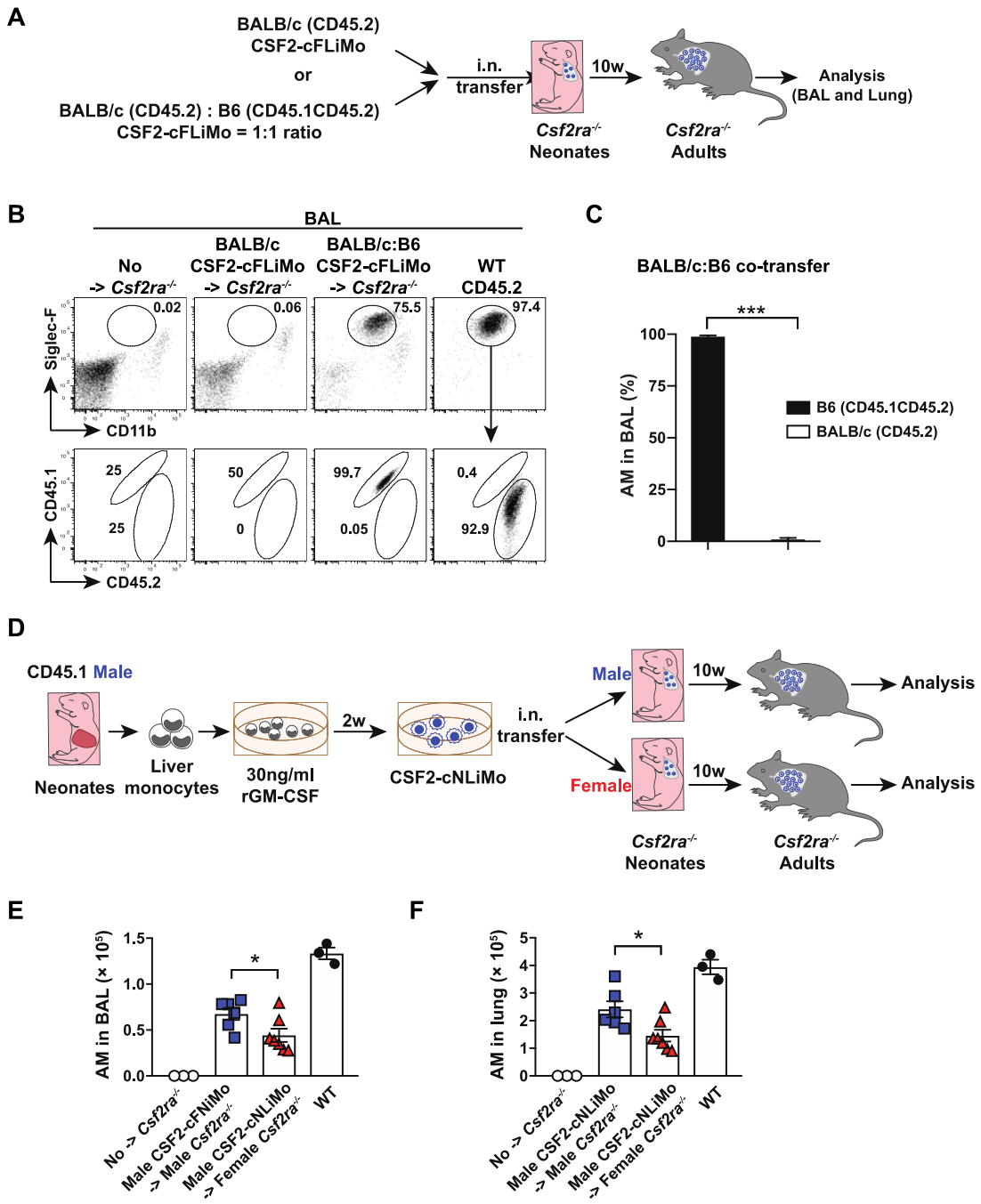
A
BALB/c (CD45.2)
CSF2-cFLiMo
or
BALB/c (CD45.2) : B6 (CD45.1CD45.2)
CSF2-cFLiMo = 1:1 ratio
i.n.
transfer
10w
Csf2ra-/-
Neonates
Csf2ra-/-
Adults
Analysis
(BAL and Lung)
B
BAL
No
-> Csf2ra-/-
BALB/c
CSF2-cFLiMo
-> Csf2ra-/-
BALB/c:B6
CSF2-cFLiMo
-> Csf2ra-/-
WT
CD45.2
Siglec-F
CD11b
CD45.1
CD45.2
0.02
0.06
75.5
97.4
25
25
50
0
99.7
0.05
0.4
92.9
C
BALB/c:B6 co-transfer
***
AM in BAL (%)
100
75
50
25
0
B6 (CD45.1CD45.2)
BALB/c (CD45.2)
D
CD45.1 Male
Neonates
Liver
monocytes
30ng/ml
rGM-CSF
2w
CSF2-cNLiMo
i.n.
transfer
Male
Female
10w
10w
Analysis
Analysis
Csf2ra-/-
Neonates
Csf2ra-/-
Adults
E
AM in BAL (× 10^5)
1.5
1.0
0.5
0.0
*
No -> Csf2ra-/-
Male CSF2-cFNiMo
-> Male Csf2ra-/-
Male CSF2-cNLiMo
-> Female Csf2ra-/-
WT
F
AM in lung (× 10^5)
5
4
3
2
1
0
*
No -> Csf2ra-/-
Male CSF2-cNLiMo
-> Male Csf2ra-/-
Male CSF2-cNLiMo
-> Female Csf2ra-/-
WT

Figure 7

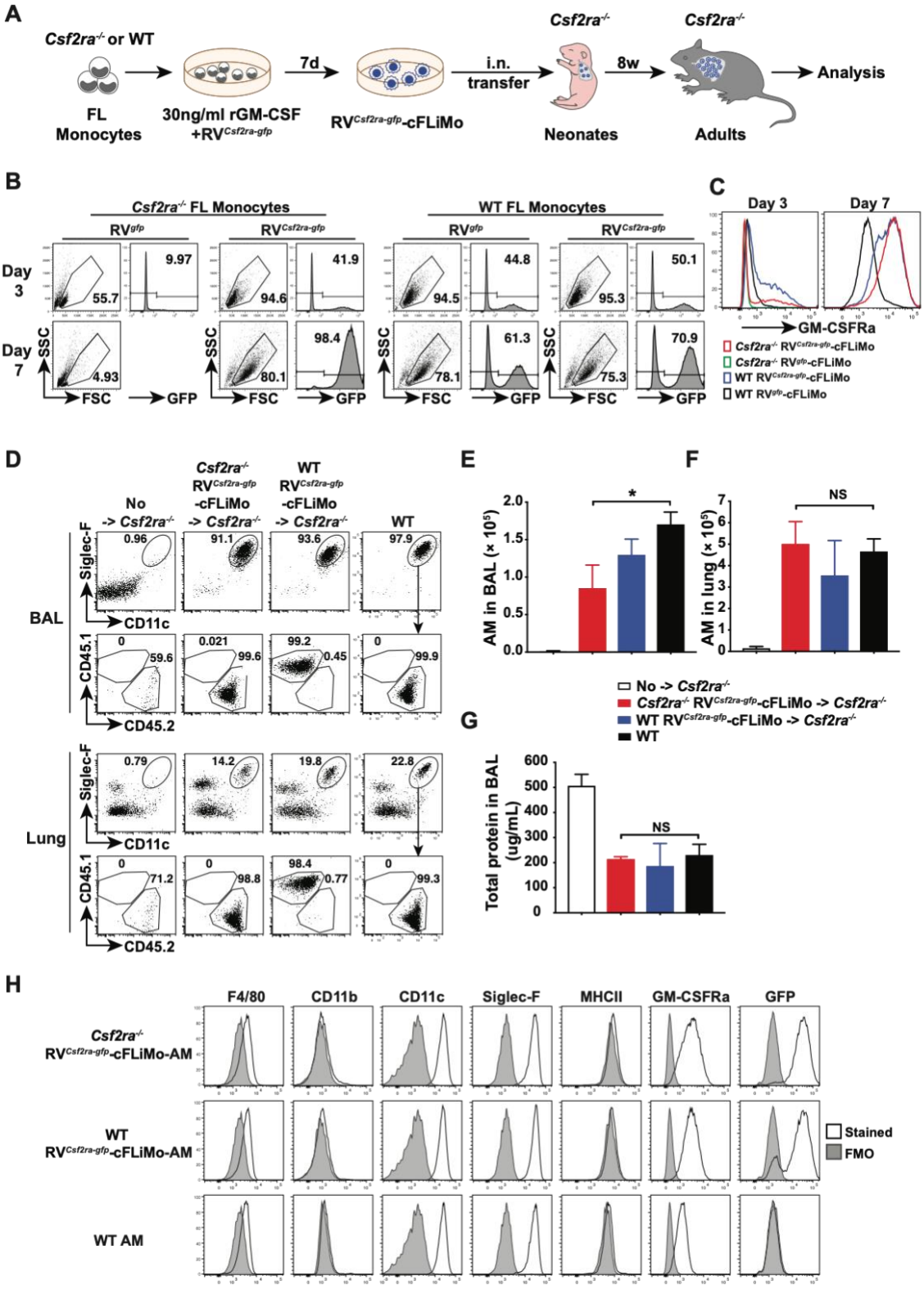
A
Csf2ra-/- or WT
FL Monocytes
30ng/ml rGM-CSF +RVCsf2ra-gfp
7d
RVCsf2ra-gfp-cFLiMo
i.n. transfer
Csf2ra-/-
Neonates
8w
Csf2ra-/-
Adults
Analysis
B
Csf2ra-/- FL Monocytes
WT FL Monocytes
RVgfp
RVCsf2ra-gfp
Day 3
Day 7
SSC
FSC
GFP
C
Day 3
Day 7
GM-CSFRa
Csf2ra-/- RVCsf2ra-gfp-cFLiMo
Csf2ra-/- RVgfp-cFLiMo
WT RVCsf2ra-gfp-cFLiMo
WT RVgfp-cFLiMo
D
No -> Csf2ra-/-
Csf2ra-/- RVCsf2ra-gfp -cFLiMo -> Csf2ra-/-
WT RVCsf2ra-gfp -cFLiMo -> Csf2ra-/-
WT
BAL
Lung
Siglec-F
CD11c
CD45.1
CD45.2
E
AM in BAL (× 10^5)
F
AM in lung (× 10^5)
NS
No -> Csf2ra-/-
Csf2ra-/- RVCsf2ra-gfp-cFLiMo -> Csf2ra-/-
WT RVCsf2ra-gfp-cFLiMo -> Csf2ra-/-
WT
G
Total protein in BAL (ug/mL)
NS
H
F4/80
CD11b
CD11c
Siglec-F
MHCII
GM-CSFRa
GFP
Csf2ra-/- RVCsf2ra-gfp-cFLiMo-AM
WT RVCsf2ra-gfp-cFLiMo-AM
WT AM
Stained
FMO